Am J Cancer Res 2018;8(1):170-182
www.ajcr.us /ISSN:2156-6976/ajcr0067866

Original Article

HOXD-AS1 promotes cell proliferation, migration and invasion through miR-608/FZD4 axis in ovarian cancer

Yanyan Wang, Wenjuan Zhang, Yuyan Wang, Shanfeng Wang

Department of Gynecology and Obstetrics, The First Affiliated Hospital of Jinzhou Medical University, Jinzhou 121000, China

Received October 24, 2017; Accepted November 1, 2017; Epub January 1, 2018; Published January 15, 2018

Abstract: Evidence is accumulating that long non-coding RNAs (lncRNAs) exert crucial roles in the incidence and progression of tumors. HOXD cluster antisense RNA 1 (HOXD-AS1), a cancer-related lncRNA, has been frequently reported to be involved in tumorigenesis and dysregulated in multiple types of human cancers; however, little is known about its role in ovarian cancer (OC). This study aimed to explore the role of HOXD-AS1 in OC and elucidate the potential mechanism involved. In the current study, HOXD-AS1 was observed to be upregulated in both OC tissues and cell lines. Besides, elevated expression of HOXD-AS1 was found to be associated with poor prognosis of OC patients. Furthermore, functional studies demonstrated that HOXD-AS1 promoted OC cell proliferation and colony formation, and enhanced the migration and invasion capabilities of OC cells. Mechanistically, HOXD-AS1 was detected to positively regulate the expression of frizzled family receptor 4 (FZD4) by competitively binding to miR-608. Taken together, HOXD4-AS1 exerts tumor-promoting functions through miR-608/FZD4 axis in OC. Our findings indicate that HOXD-AS1 may be used as a promising therapeutic target and a novel prognostic biomarker for OC.

Keywords: HOXD-AS1, miR-608, FZD4, ovarian cancer

Introduction

Ovarian cancer (OC) is the most fatal gynecological malignancy and the fourth leading cause of cancer-related deaths among women [1, 2]. It was estimated that 22,280 new cases of OC were diagnosed and 14,240 patients died from OC in the United States in 2016 [3]. The high mortality is partially attributed to the fact that the early-stage OC is mostly asymptomatic [4-6]. Although conventional therapeutic strategies have been developed, the long-term prognosis of OC patients is still poor. Therefore, novel and effective therapeutic approaches are in urgent demand.

Long non-coding RNAs (lncRNAs) are a large type of mRNA-like non-coding transcripts longer than 200 nucleotides, which do not serve as templates for protein synthesis [7, 8]. Besides, LncRNAs are expressed in tissue-specific and time-specific manners. Recently, lncRNAs have gained increasing attention and been reported to be implicated in a wide range of human cancers [9-11]. Accumulating evidence has revealed that lncRNAs may exert their roles in tumorigenesis by competitively binding to cancer-related microRNAs (miRNAs) [12-14]. Antisense long non-coding RNAs (aslncRNAs) are a class of lncRNAs that are oriented in the antisense direction relative to protein-coding mRNA transcripts [15, 16].

It is acknowledged that HOXD is a member of homeobox (HOX) gene family, which plays crucial roles in the development of embryos and organs [17, 18]. HOXD cluster antisense RNA 1 (HOXD-AS1), a novel lncRNA, is transcribed from the HOXD gene cluster located on human chromosome 2q31.2 in an antisense manner. Increasing evidence has revealed that ectopic expression of HOXD-AS1 is involved in the occurrence and progression of diverse types of human tumors, including hepatocellular carcinoma, bladder cancer, prostate cancer, neuroblastoma and gastric cancer [19-23]; however, its role in OC remains to be elucidated.

The present study aimed to explore the role of HOXD-AS1 in OC and clarify the potential molec-

ular mechanisms involved. In the current study, we found HOXD-AS1 was notably upregulated in OC tissues and cell lines. Moreover, functional studies showed that HOXD-AS1 promoted OC cell proliferation, migration and invasion. Additionally, mechanistic studies demonstrated that HOXD-AS1 exerts tumor-promoting roles through miR-608/FZD4 axis in OC.

Materials and methods

Patients and tissue samples

OC tissues and the corresponding adjacent non-cancerous tissues were obtained from 16 patients in the First Affiliated Hospital of Jinzhou Medical University (Jinzhou, China) from February 2014 to December 2016. Corresponding adjacent normal tissues were obtained at a distance of 5 cm from OC tissues. All clinical specimens were immediately frozen in liquid nitrogen and stored at -80°C for further experiments. This study was carried out in accordance with the guidelines by the Ethics and Scientific Committee of Jinzhou Medical University. Written informed consent was obtained from all patients enrolled in the current study.

Cell culture

Three human OC cell lines (Caov-3, SK-OV-3 and OVCAR-3) and a normal human ovary cell line (IOSE80) were obtained from Shanghai Cell Bank, Chinese Academy of Sciences (Shanghai, China). These cells were cultured in DMEM medium (Gibco, Grand Island, New York, USA) supplemented with 10% fetal bovine serum (FBS, Sigma-Aldrich, St. Louis, MO, USA). All the cells were maintained at 37°C in a humidified incubator with 5% CO_2.

RNA extraction and quantitative real-time polymerase chain reaction (qRT-PCR)

Total RNA and microRNAs were extracted from tissues and cells using TRIzol reagent (Qiagen, Hilden, Germany) according to the manufacturer's protocol. Following quantification by Nanodrop 2000 (Thermo Fisher Scientific, Waltham, USA), the extracted total RNA was reverse-transcribed using Reverse Transcription Kit (Takara, Dalian, China). RT-PCR was performed on an Applied Biosystems 7500 Fast Real-Time PCR systems (Applied Biosystems). The specific primer sequences synthesized by Shanghai Sangon Biological Engineering Technology and Service were as followed: HOXD-AS1, forward 5'-GGCTCTTCCCTAATGTGTGG-3' and reverse 5'-CAGGTCCAGCATGAAACAGA-3'; FZD4, forward 5'-GGTGGCTCCCCTCTTTACTT-3', reverse 5'-ATCACACACGTTGCAGAAC-3'; GAPDH, forward 5'-ACAACTTTGGTATCGTGGAAGG-3', reverse 5'-GCCATCACGCCACAGTTTC-3'. The PCR conditions were as follows: denaturation at 95°C for 10 min, followed by 40 cycles of 95°C for 5 sec and 60°C for 40 sec. GAPDH was used as an endogenous control to normalize HOXD-AS1 and FZD4 expression levels. The relative expression level was calculated using the $2^{-\Delta\Delta Ct}$ method. The experiments were performed in triplicate.

Cell transfection

Cell transfection was performed using Lipofectamine 2000 (Invitrogen, Waltham, USA) according to manufacturer's instructions. Cells (5×10^5 cells/well in six-well plates, 70%~80% confluency) were transfected with HOXD-AS1 mimics or si-HOXD-AS1. HOXD-AS1 mimics and small interfering RNA to knockdown HOXD-AS1 were synthesized by Shanghai GenePharma Co., Ltd. (Shanghai, China). Small interfering RNA sequences were listed as followed: si-HOXD-AS1 sense, 5'-GAAAGAAGGACCAAAGTAA-3'; si-HOXD-AS1 antisense, 5'-GCACAAAGGAACAAGGAAA-3'. Cells were harvested 48 h post-transfection for further experiments.

Cell viability assay

Cell proliferation was assessed using MTT Cell Proliferation and Cytotoxicity Assay Kit (Sigma-Aldrich, St. Louis, USA) according to the manufacturer's instructions. In brief, cells were seeded in each well of a 96-well plate at a density of 1×10^4 cells/well. Following incubation at 37°C for different periods of time (0, 24, 48 and 72 h), the culture medium was removed and MTT (20 μl; 5 mg/mL) was added to each well. After incubation at 37°C for another 4 hours, MTT solution was removed and replaced with dimethyl sulfoxide (DMSO; 150 μl, 4%; Sigma-Aldrich). Absorbance was measured at 560 nm by a microplate reader (Bio-Tek Instruments, Germany).

Colony formation assay

Colony formation assays were performed to evaluate the clonogenic ability of OC cells. Briefly, 400 cells from each treatment were

allowed to grow for two weeks on 6-well culture plates to form colonies. Crystal violet (2%) was used to stain colonies and the number of colonies was subsequently counted under an invert microscope (Olympus, Japan). The experiments were performed in triplicate.

Wound healing assay

Cells were seeded in 6-well culture plates to grow into a monolayer (basically 100% confluence). The cell monolayer was scraped using pipette and washed twice with medium to form a wound. The cells were further cultured in the medium for 24 h and closure of scratch was observed using a inverted microscope (Olympus). Cells were observed at 0 and 24 h after scraping under an inverted microscope and corresponding photographs were taken. The cell-free area at 24 h after wounding and original denuded area were measured using the Image J software (National Institutes of Health, Bethesda, MD, USA).

Transwell invasion assay

Transwell invasion assay was performed to assess cell invasion. The upper surface of the a filter (pore size, 8.0 μm; Biosciences, Heidelberg, Germany) was coated with basement membrane Matrigel (BD Bioscience), at a concentration of 2 mg/ml and incubated at 4°C for 3 h. 2×10^4 cells were seeded into upper chamber with 200 μl serum-free medium. The lower chamber was supplemented with 750 μl medium containing 10% FBS. Following incubation for 24 h at 37°C, cells were fixed with 4% polyoxymethylene and stained with 0.5% crystal violet (Sigma-Aldrich). Then stained cells were observed and counted under a microscope. Five visual fields were selected and the average number was taken.

Luciferase reporter assay

Wild-type HOXD-AS1, mutant HOXD-AS1 were inserted into pmirGLO reporter vectors (Promega, Madison, WI, USA), respectively. OVCAR-3 cells were co-transfected with miR-608 mimics and wild-type HOXD-AS1 or mutant HOXD-AS1 by Lipofectamine 2000 (Invitrogen). Relative luciferase activity was measured on a dual-luciferase reporter assay system (Promega) at 48 h post-transfection. Data were expressed as the ratio of Renilla luciferase activity to firefly luciferase activity. Luciferase reporter assays to validate the direct binding of miR-608 to FZD4 3'UTR were performed as described above.

RNA-binding protein immunoprecipitation (RIP)

RIP assays were performed using EZ-Magna RIP™ RNA-Binding Protein Immunoprecipitation Kit (Millipore, Billerica, MA, USA) according to manufacturer's protocol. Briefly, RIP buffer containing magnetic beads conjugated with human anti-Ago2 antibody (Millipore) or negative control IgG (Millipore) was added to cell lysate and incubated for overnight at 4°C. Proteinase K was used to digest the protein and then the co-precipitated RNAs were isolated. The purified RNAs were subject to RT-PCR analysis.

Western blot analysis

Protein lysates were extracted from cells using 500 μl radio immunoprecipitation assay (RIPA) buffer with 1 mM phenylmethane sulfonyl fluoride. Samples were subsequently sonicated for 2 min and centrifuged. The supernatants were collected and used for protein analysis. Lysates were separated on 8% polyacrylamide gels and transferred onto PVDF membrane. The membranes were blocked with phosphate-buffered saline (PBS) containing 0.1% Tween-20 (PBST) and 5% nonfat milk (w/v) for 1 h at room temperature. After they were washed with PBST, the membranes were probed with antibodies overnight at 4°C. Anti-FZD4 (ab83042) and anti-GAPDH (ab8245) were obtained from Abcam (Cambridge, MA, USA) and used at the following dilutions: anti-FZD4 (1:1000) and anti-GAPDH (1:3000). The membranes were washed again with PBST, then horseradish peroxidase (HRP) labeled IgG at 1:5000 dilution was added at room temperature for 1 h, and the blots were developed using ECL Western blotting reagents.

Statistical analysis

Data were expressed as mean ± standard deviation (SD). Statistical analysis was performed using SPSS 16.0 software (SPSS, Chicago, IL, USA). Kaplan-Meier survival and log-rank test were used for survival analysis and comparison of differences in overall survival. Correlation between HOXD-AS1 expression and miR-608 or FZD4 expression in OC tissues was determined using Pearson's correlation analysis. Two-tailed student's *t*-test was applied to compare the differences between two groups and

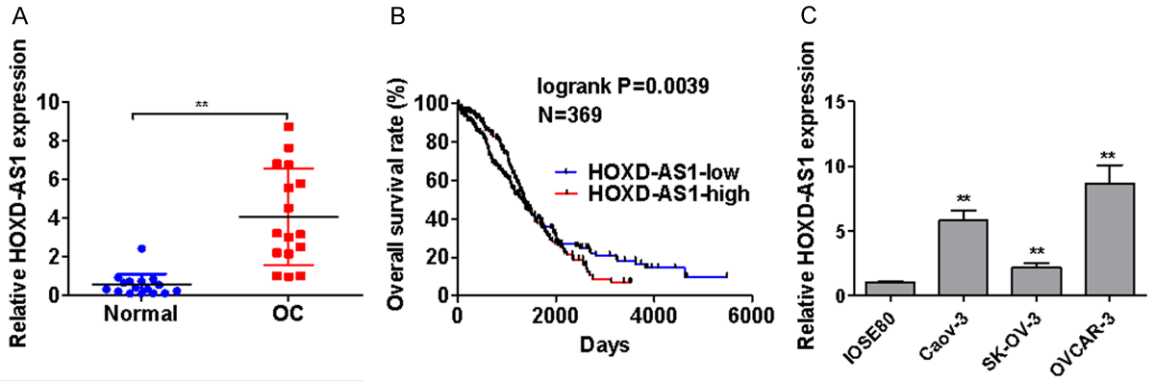

Figure 1. HOXD-AS1 is significantly upregulated in OC tissues and cell lines. A. Relative expression levels of HOXD-AS1 in 16 pairs of OC tissues and adjacent noncancerous tissues were identified using qRT-PCR. B. Information on 369 cases with OC was downloaded from TCGA database. Patients were divided into high HOXD-AS1 expression group and low HOXD-AS1 expression group on the basis of the median of HOXD-AS1 expression levels in OC tissues. Kaplan-Meier survival analysis and log-rank test were applied to evaluate the correlation between HOXD-AS1 expression levels and overall survival rate. C. Relative expression levels of HOXD-AS1 in normal ovary cell line IOSE80 and three OC cell lines (Caov-3, SK-OV-3 and OVCAR-3). $**P<0.01$. HOXD-AS1, HOXD homeobox gene cluster antisense RNA 1; OC, ovarian cancer. TCGA, the cancer genome atlas.

one-way analysis of variance (ANOVA) followed by Dunnett's multiple comparison was employed to compare the differences among three independent groups. $P<0.05$ was considered statistically significant.

Results

HOXD-AS1 is significantly upregulated in OC tissues and cell lines

Even though HOXD-AS1 has been frequently reported to be involved in the oncogenesis and progression of diverse types of human cancers, its role in OC remains unclear. Initially, we performed qRT-PCR analysis to examine the expression of HOXD-AS1 in 16 pairs of OC tissues and matched adjacent noncancerous tissues. As evident from qRT-PCR analysis, OC tissues exhibited higher expression levels of HOXD-AS1 than paracancerous tissues (**Figure 1A**). To investigate the association between increased HOXD-AS1 expression and the prognosis of OC patients, we analyzed the information of 369 patients downloaded from TCGA online database. Patients with high HOXD-AS1 expression were discovered to experience lower overall survival rate compared with those with low HOXD-AS1 expression (**Figure 1B**). Consistently, HOXD-AS1 was significantly upregulated in OC cell lines (Caov-3, SK-OV-3 and OVCAR-3) compared with normal ovary cell line IOSE80 (**Figure 1C**). OVCAR-3 cells (highest endogenous HOXD-AS1 expression) were selected for subsequent experiments. The findings indicate that elevated expression of HOXD-AS1 may be associated with poor prognosis of OC patients. Taken together, HOXD-AS1 is markedly up regulated in OC tissues and cell lines.

HOXD-AS1 promotes OC cell proliferation and colony formation

To explore the potential role of HOXD-AS1 in OC, OVCAR-3 cells were transfected with HOXD-AS1 mimics or siRNA-HOXD-AS1. The transfection efficiency was identified using qRT-PCR (**Figure 2A**). As presented in **Figure 2B**, OVCAR-3 cell proliferation was dramatically accelerated by HOXD-AS1 mimics compared with negative control group, whereas HOXD-AS1 knockdown markedly suppressed OVCAR-3 cell proliferation. As evident from colony formation assay, HOXD-AS1 overexpression markedly enhanced clonogenic ability of OVCAR-3 cells; in addition, clonogenic capability of OVCAR-3 cells was notably repressed by HOXD-AS1 downregulation (**Figure 2C**). These results indicate that HOXD-AS1 promotes OC cell proliferation and colony formation.

HOXD-AS1 accelerates OC cell migration and invasion

To determine whether HOXD-AS1 influences the mobility of OC cells, we evaluated the migration and invasion capabilities of OVCAR-3 cells after transfection with HOXD-AS1 mimics or si-HOXD-AS1. As obvious from would healing

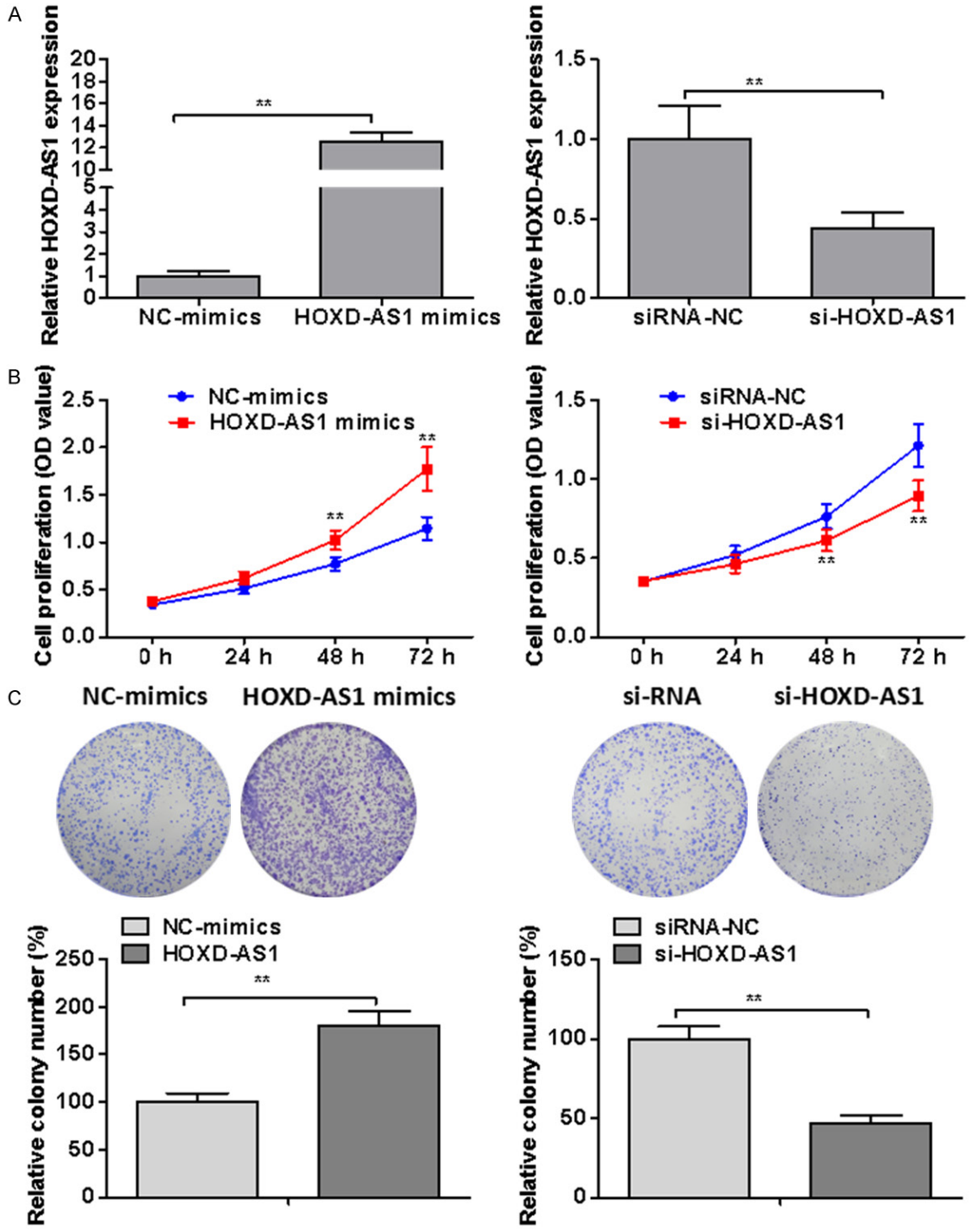

Figure 2. HOXD-AS1 promotes OC cell proliferation and colony formation. A. HOXD-AS1 expression levels were identified using qRT-PCR after transfection with HOXD-AS1 mimics or si-HOXD-AS1. B. Cell proliferation was identified using MTT assay after transfection with HOXD-AS1 mimics or si-HOXD-AS1. C. Clonogenic ability was assessed by colony formation assays after transfection with HOXD-AS1 mimics or si-HOXD-AS1. $^{**}P<0.01$. HOXD-AS1, HOXD homeobox gene cluster antisense RNA 1; OC, ovarian cancer; siRNA, small interfering RNA; NC, negative control.

assays, HOXD-AS1 overexpression markedly enhanced the migration ability of OVCAR-3 cells compared with negative control group, whereas migration capability of OVCAR-3 cells was dra-

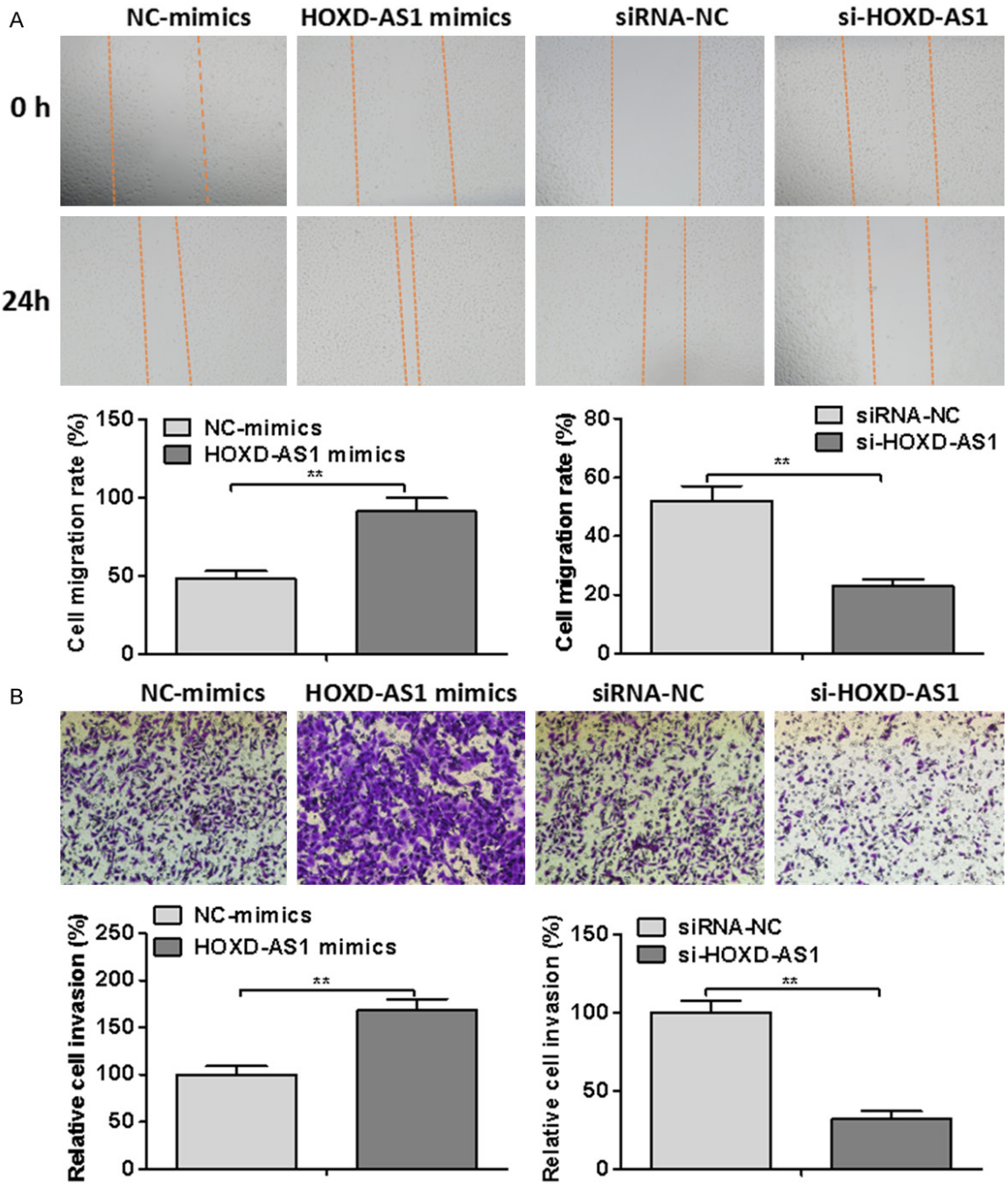

Figure 3. HOXD-AS1 promotes OC cell migration and invasion. A. Cell migration was assessed using would healing assays. B. Cell invasion was evaluated by transwell invasion assays. ***P*<0.01. HOXD-AS1, HOXD homeobox gene cluster antisense RNA 1; OC, ovarian cancer; siRNA, small interfering RNA; NC, negative control.

matically inhibited by HOXOD-AS1 knockdown (**Figure 3A**). Transwell invasion assays demonstrated that OVCAR-3 cell invasion was remarkably promoted by HOXD-AS1 mimics compared with negative control group, besides, HOXD-AS1 downregulation significantly repressed OVCAR-3 cell migration (**Figure 3B**). Our findings indicate that HOXD-AS1 accelerates OC cell migration and invasion.

HOXD-AS1 interacts with miR-608 in OC cells

Mounting studies have showed that lnc RNAs may be involved in the pathogenesis and devel-

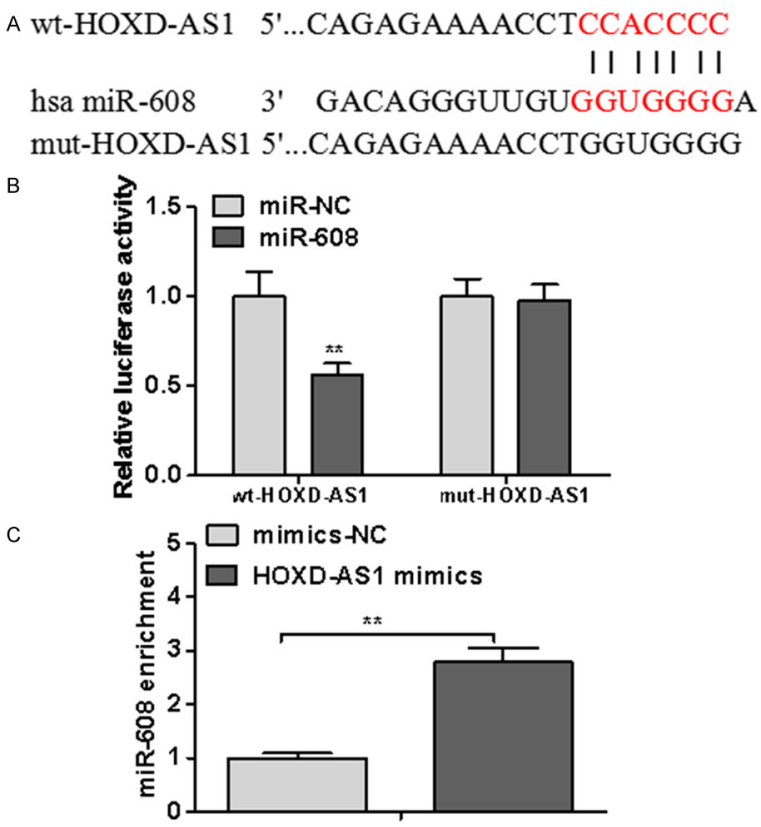

Figure 4. HOXD-AS1 interacts with miR-608 in OC cells. A. A putative binding site of miR-608 in HOXD-AS1 was predicted by miRanda algorithm. B. Luciferase activity was detected after co-transfection with miR-608 and wt-HOXD-AS1 or mut-HOXD-AS1. C. Anti-Ago2 RIP was performed to enrich miRNAs interacted with HOXD-AS1 in OVCAR-3 cells after transfection with mimics-NC or HOXD-AS1 mimics, followed by qRT-PCR to detect miR-608 levels in the immunoprecipitates. $^{**}P<0.01$. HOXD-AS1, HOXD homeobox gene cluster antisense RNA 1; OC, ovarian cancer; wt, wild-type; mut, mutant; Ago2, argonaute 2, RIP, RNA immunoprecipitation.

opment of various human tumors via competitive binding to miRNAs. To elucidate the underlying mechanisms by which HOXD-AS1 promotes OC cell proliferation, migration and invasion. We applied miRanda algorithm to predict the potential targets of HOXD-AS1. miR-608, frequently reported to be involved in multiple types of human cancers, was selected as a candidate target of HOXD-AS1 (**Figure 4A**). Furthermore, we constructed luciferase reporters containing the predicted miR-608 binding site (wt-HOXD-AS1) and its corresponding mutant site (mut-HOXD-AS1). As presented in **Figure 4B**, co-transfection of miR-608 and wt-HOXD-AS1 markedly decreased the luciferase activity, while co-transfection with miR-608 and mut-HOXD-AS1 did not change the luciferase activity. To confirm the interaction between HOXD-AS1 and miR-608, anti-Ago2 RIP assays were performed to pull down endogenous miRNAs interacted with HOXD-AS1 in OVCAR-3 cells. MiR-608 was observed to be significantly enriched by HOXD-AS1 mimics treatment compared with negative control group (**Figure 4C**). These results suggest that HOXD-AS1 interacts with miR-608 in OC cells.

HOXD-AS1 upregulates FZD4 expression by competitively binding to miR-608 in OC cells

Recent studies have demonstrated that lncRNAs may serve as competing endogenous RNAs (ceRNAs) through competitively binding to shared miRNAs. As presented in **Figure 5A**, HOXD-AS1 mimics significantly downregulated miR-608 expression in OVCAR-3 cells compared with negative control group, whereas knockdown of HOXD-AS1 upregulated miR-608 expression in OVCAR-3 cells. To further elucidate the molecular mechanism by which HOXD-AS1 exerts its promotive effects on OC proliferation, migration and invasion, the potential targets of miR-608 were predicted using miRanda online software. Among the predicted targets, FZD4 arose our interest for its importance in carcinogenesis and progression of a wide range of human tumors, and was selected as a candidate target of miR-608 (**Figure 5B**). Luciferase reporter assays were performed to validate the direct binding of miR-608 to FZD4 3'UTR. As illustrated in **Figure 5C**, co-transfection of miR-608 and wild-type FZD4 3'UTR significantly repressed the activity of luciferase in comparison with negative control group, whereas co-transfection of miR-608 and mutant FZD4 3'UTR failed to suppress luciferase activity. RT-PCR analysis and Western blotting analysis revealed that FZD4 was dramatically downregulated by miR-608 mimics (**Figure 5D** and **5E**).

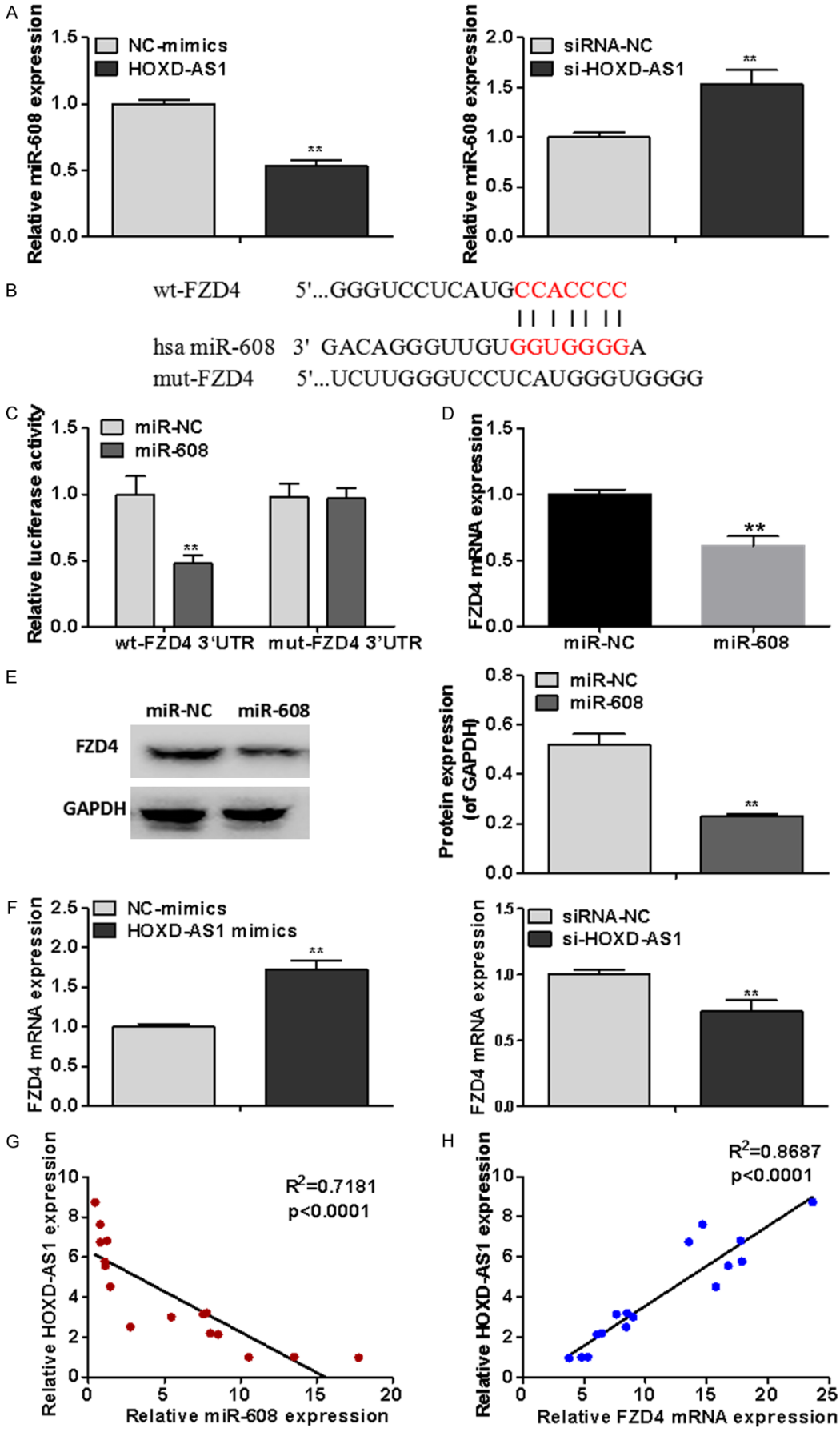
A
Relative miR-608 expression
NC-mimics
HOXD-AS1
siRNA-NC
si-HOXD-AS1
B
wt-FZD4 5'...GGGUCCUCAUGCCACCCC
hsa miR-608 3' GACAGGGUUGUGGUGGGGA
mut-FZD4 5'...UCUUGGGUCCUCAUGGGUGGGG
C
Relative luciferase activity
miR-NC
miR-608
wt-FZD4 3'UTR
mut-FZD4 3'UTR
D
FZD4 mRNA expression
E
miR-NC
miR-608
FZD4
GAPDH
Protein expression (of GAPDH)
F
NC-mimics
HOXD-AS1 mimics
G
Relative HOXD-AS1 expression
Relative miR-608 expression
R2=0.7181
p<0.0001
H
R2=0.8687
p<0.0001
Relative FZD4 mRNA expression

Figure 5. HOXD-AS1 upregulates FZD4 expression by competitively binding to miR-608 in OC cells. A. MiR-608 expression was detected by qRT-PCR after transfection with mimics-NC or HOXD-AS1 mimics. B. A putative binding site of miR-608 in FZD4 was predicted by miRanda online software. C. Luciferase activity was measured after co-transfection with miR-608 and wt-FZD4 3'UTR fragment or mut-FZD4 3'UTR fragment. D. FZD4 mRNA expression was measured by qRT-PCR after transfection with miR-608 mimics. E. FZD4 protein expression was identified using western blots. F. FZD4 mRNA expression was assessed by qRT-PCR after transfection with HOXD-AS1 mimics or si-HOXD-AS1. G. Correlation between HOXD-AS1 expression and miR-608 expression in OC tissues was determined by Pearson's correlation analysis. H. Correlation between HOXD-AS1 expression and FZD4 mRNA expression in OC tissues was determined by Pearson's correlation analysis. $^{**}P<0.01$. HOXD-AS1, HOXD homeobox gene cluster antisense RNA 1; OC, ovarian cancer; FZD4, frizzled family receptor 4; wt, wild-type; mut, mutant.

These data indicate that miR-608 directly binds to 3'UTR of FZD4 to suppress its expression.

To investigate whether HOXD-AS1 modulates the expression of FZD4, we transfected OVCAR-3 cells with HOXD-AS1 mimics or si-HOXD-AS1. As obvious from qRT-PCR analysis, FZD4 was markedly upregulated by HOXD-AS1 mimics compared with negative control group, whereas FZD4 was notably downregulated by knockdown of HOXD-AS1 (**Figure 5F**). Additionally, Pearson's correlation analysis showed that HOXD-AS1 expression was inversely correlated with miR-608 expression in OC tissues. On the contrary, HOXD-AS1 expression was positively correlated with FZD4 mRNA expression in OC tissues (**Figure 5G** and **5H**). Our findings suggest that HOXD-AS1 positively modulates the expression of FZD4 by sponging miR-608.

miR-608 mediates the effects of HOXD-AS1 on OC cell proliferation, migration and invasion

To investigate whether the promotive effects of HOXD-AS1 on OC cell proliferation, migration and invasion are mediated by miR-608, we rescued the expression of miR-608 in OVCAR-3 cells. Restoring the expression of miR-608 was noticed to partially reverse the promotive effects of HOXD-AS1 on OC cell proliferation, colony formation, migration and invasion (**Figure 6A-D**). Furthermore, qRT-PCR and Western blotting analyses demonstrated that rescuing the expression of miR-608 dramatically down-regulated the expression of FZD4 in OVCAR-3 cells (**Figure 6E** and **6F**). Our data indicate that the promotive effects of HOXD-AS1 on OC cell proliferation, migration and invasion are mediated by miR-608.

Discussion

OC, a lethal malignancy of the female reproductive system, has brought high health risks and tremendous economic pressures to the woman around the world [3, 5]. Even though conventional therapeutic strategies, such as surgery, radiotherapy and chemical therapy, have slightly improved the overall survival of OC patients, the long-term prognosis remains poor. Mounting evidence has demonstrated that lncRNAs are dysregulated in a wide range of human cancers and involved in the oncogenesis and progression [11-14]. Previous studies have revealed that aberrant expression of HOXD-AS1 is implicated in multiple types of human tumors. Wang et al discovered that HOXD-AS1 was significantly upregulated and in hepatocellular carcinoma tissues and plays a pro-metastasis role in liver cancer metastasis by regulating SOX4 [19]. Li et al demonstrated that HOXD-AS1 acted as an oncogene in the progression of bladder cancer [20]. HOXD-AS1 was found to function as an oncogene to facilitate non-small cell lung cancer progression by sequestering miR-147 [24]. Besides, HOXD-AS1 has been reported to be involved in the occurrence and development of gastric cancer, prostate cancer and neuroblastoma [21-23]. However, little is known about the role of HOXD-AS1 in OC. Thus, a better understanding of the biological functions of HOXD-AS1 may be useful for developing promising therapeutic strategies and identifying novel prognostic biomarkers.

In the current study, we initially examined the expression of HOXD-AS1 in 16 pairs of OC tissues and matched adjacent normal tissues and found that HOXD-AS1 was markedly upregulated in OC tissues. Furthermore, we downloaded the information of 369 OC patients from TCGA online database in order to investigate the association between HOXD-AS1 expression and the prognosis of OC patients. Kaplan-Meier survival analysis revealed that patients with high HOXD-AS1 expression experienced lower overall survival rate. Consistently, HOXD-AS1 was notably upregulated in OC cell lines. To better understand the role of HOXD-AS1 in OC, func-

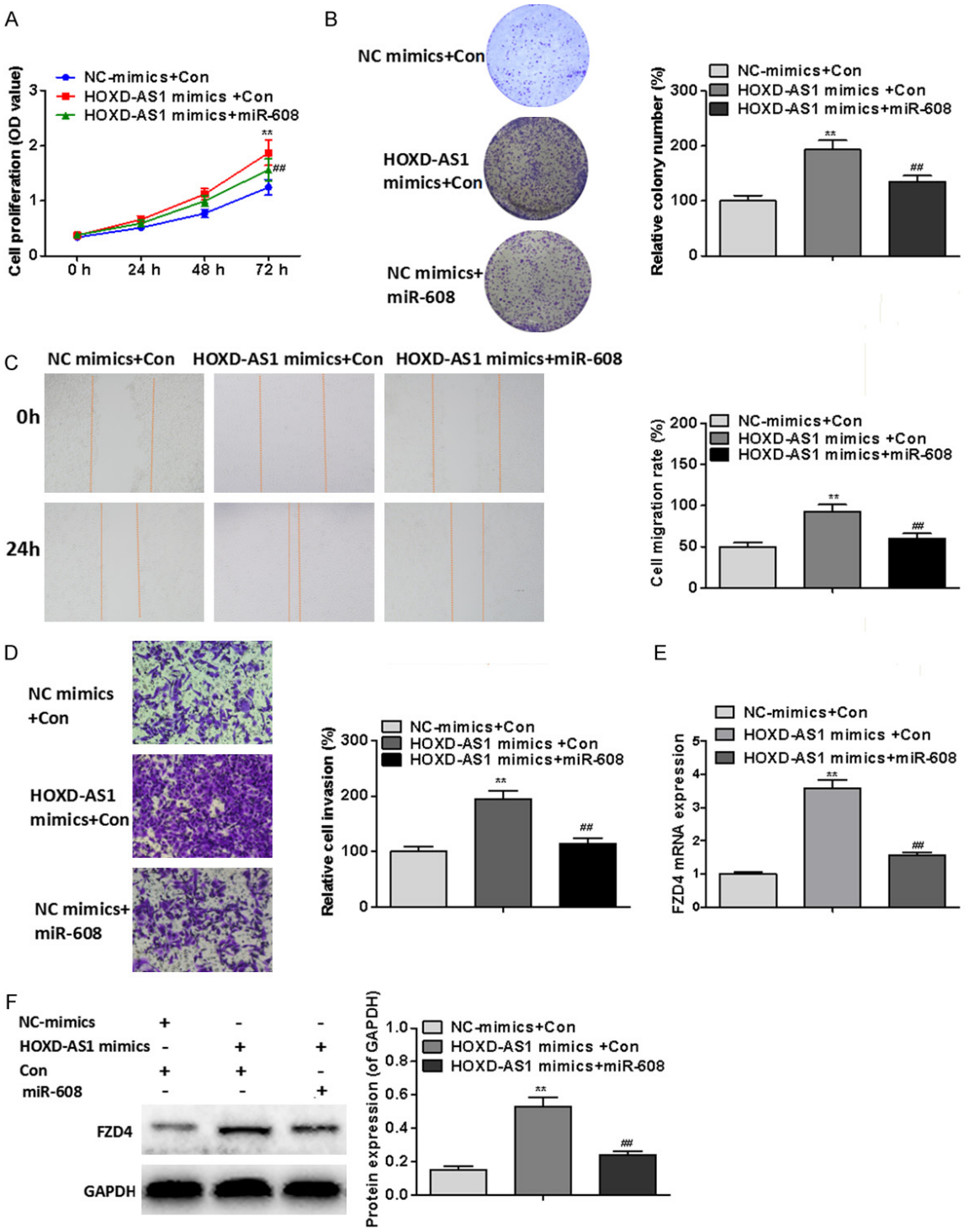

Figure 6. miR-608 mediates the effects of HOXD-AS1 on OC cell proliferation, migration and invasion. A. Cell proliferation was assessed by MTT assays after rescuing the expression of miR-608. B. Clonogenic ability was identified by colony formation assays after rescuing the expression of miR-608. C. Cell migration was measured by wound healing assays. D. Cell invasion was evaluated by transwell invasion assay after rescuing the expression of miR-608. E. FZD4 mRNA expression was examined using qRT-PCR after rescuing the expression of miR-608. F. FZD4 protein expression was analyzed by western blots after rescuing the expression of miR-608. **P<001 vs NC mimics+Con group, $^{\#\#}P$<0.01 vs HOXD-AS1 mimics+miR-608. HOXD-AS1, HOXD homeobox gene cluster antisense RNA 1; OC, ovarian cancer; NC, negative control.

tional studies were conducted. Our data demonstrated that HOXD-AS1 overexpression facilitated OC cell proliferation, enhanced the clonogenic ability of OC cells, and accelerated OC cell migration and invasion. Our findings reveal that HOXD-AS1 may function as an oncogene in OC.

Evidence is accumulating that lncRNAs are involved in carcinogenesis and progression as competing endogenous RNAs (ceRNAs) by sponging miRNAs [25, 26]. Previous studies have demonstrated that miR-608 served as an tumor suppressor in various types of human tumors, including colon cancer, colorectal cancer, glioma and bladder cancer [27-30]. FZD4, a member of frizzled (FZD) receptor family, has been reported to function as the membrane receptor for Wnt signaling glycoproteins and implicated in the progression of human tumors [31-34]. To explore the underlying molecular mechanisms by which HOXD-AS1 exerts an oncogenic role in OC, bioinformatics analysis and luciferase reporter assays revealed that HOXD-AS1 could competitively bind to miR-608 in OVCAR-3 cells. In addition, FZD4 was identified as a direct of miR-608 in OVCAR-3 cells. Moreover, HOXD-AS1 was observed to upregulate the expression of FZD4 by competitively sponging miR-608 in OVCAR-3 cells. It was noted that HOXD-AS1 expression was negatively correlated to miR-608 expression, but positively correlated to FZD4 mRNA expression in OC tissues.

To further elucidate the mechanisms underlying OC oncogenesis and progression, we rescued the miR-608 in the OVCAR-3 cells. Rescuing the expression of miR-608 was found to partially inverse the promotive effects of HOXD-AS1 on OC cell proliferation, colony formation, migration and invasion. Besides, rescuing the expression was noticed to down-regulate the expression of FZD4. These results demonstrated that indicate that the promotive effects of HOXD-AS1 on OC cell proliferation, colony formation, cell migration and invasion were mediated partially by miR-608/FZD4 axis.

In conclusion, HOXD-AS is significantly upregulated in OC tissues and cell lines, and exerts oncogenic roles in OC partially through miR-608/FZD4 axis. Our study provides new insights into the potential molecular mechanisms underlying OC carcinogenesis and progression. Thus, HOXD-AS1 may be used as a promising therapeutic target and a novel prognostic biomarker for OC.

Disclosure of conflict of interest

None.

Address correspondence to: Shanfeng Wang, Department of Gynecology and Obstetrics, The First Affiliated Hospital of Jinzhou Medical University, No. 2 Section 5 Renmin Street, Jinzhou 121000, China. E-mail: sfwang1020@163.com

References

[1] Smolle E, Taucher V, Petru E, and Haybaeck J. Targeted treatment of ovarian cancer--the multiple - kinase - inhibitor sorafenib as a potential option. Anticancer Res 2014; 34: 1519-1530.

[2] Yoneda A, Lendorf ME, Couchman JR and Multhaupt HA. Breast and ovarian cancers: a survey and possible roles for the cell surface heparan sulfate proteoglycans. J Histochem Cytochem 2012; 60: 9-21.

[3] Siegel RL, Miller KD and Jemal A. Cancer statistics, 2016. CA Cancer J Clin 2016; 66: 7-30.

[4] Fishman DA, Cohen L, Blank SV, Shulman L, Singh D, Bozorgi K, Tamura R, Timor-Tritsch I and Schwartz PE. The role of ultrasound evaluation in the detection of early-stage epithelial ovarian cancer. Am J Obstet Gynecol 2005; 192: 1214-1222.

[5] Goonewardene TI, Hall MR and Rustin GJ. Management of asymptomatic patients on follow-up for ovarian cancer with rising CA-125 concentrations. Lancet Oncol 2007; 8: 813-821.

[6] Reade CJ, Riva JJ, Busse JW, Goldsmith CH and Elit L. Risks and benefits of screening asymptomatic women for ovarian cancer: a systematic review and meta-analysis. Gynecol Oncol 2013; 130: 674-681.

[7] Bakhtiarizadeh MR, Hosseinpour B, Arefnezhad B, Shamabadi N and Salami SA. In silico prediction of long intergenic non-coding RNAs in sheep. Genome 2016; 59: 263-275.

[8] Angrand PO, Vennin C, Le Bourhis X and Adriaenssens E. The role of long non-coding RNAs in genome formatting and expression. Front Genet 2015; 6: 165.

[9] Liu XH, Sun M, Nie FQ, Ge YB, Zhang EB, Yin DD, Kong R, Xia R, Lu KH, Li JH, De W, Wang KM and Wang ZX. Lnc RNA HOTAIR functions as a competing endogenous RNA to regulate HER2 expression by sponging miR-331-3p in gastric cancer. Mol Cancer 2014; 13: 92.

[10] Li H, Yu B, Li J, Su L, Yan M, Zhu Z and Liu B. Overexpression of lncRNA H19 enhances car-

cinogenesis and metastasis of gastric cancer. Oncotarget 2014; 5: 2318-2329.
[11] Xiang JF, Yin QF, Chen T, Zhang Y, Zhang XO, Wu Z, Zhang S, Wang HB, Ge J, Lu X, Yang L and Chen LL. Human colorectal cancer-specific CCAT1-L lncRNA regulates long-range chromatin interactions at the MYC locus. Cell Res 2014; 24: 513-531.
[12] Gao S, Wang P, Hua Y, Xi H, Meng Z, Liu T, Chen Z and Liu L. ROR functions as a ceRNA to regulate Nanog expression by sponging miR-145 and predicts poor prognosis in pancreatic cancer. Oncotarget 2016; 7: 1608-1618.
[13] Shao Y, Ye M, Li Q, Sun W, Ye G, Zhang X, Yang Y, Xiao B and Guo J. LncRNA-RMRP promotes carcinogenesis by acting as a miR-206 sponge and is used as a novel biomarker for gastric cancer. Oncotarget 2016; 7: 37812-37824.
[14] Zhang D, Cao C, Liu L and Wu D. Up-regulation of lncRNA SNHG20 predicts poor prognosis in hepatocellular carcinoma. J Cancer 2016; 7: 608-617.
[15] Zucchelli S, Cotella D, Takahashi H, Carrieri C, Cimatti L, Fasolo F, Jones MH, Sblattero D, Sanges R, Santoro C, Persichetti F, Carninci P and Gustincich S. SINEUPs: a new class of natural and synthetic antisense long non-coding RNAs that activate translation. RNA Biol 2015; 12: 771-779.
[16] Yuan SX, Tao QF, Wang J, Yang F, Liu L, Wang LL, Zhang J, Yang Y, Liu H, Wang F, Sun SH and Zhou WP. Antisense long non-coding RNA PCNA-AS1 promotes tumor growth by regulating proliferating cell nuclear antigen in hepatocellular carcinoma. Cancer Lett 2014; 349: 87-94.
[17] Manohar CF, Salwen HR, Furtado MR and Cohn SL. Up-regulation of HOXC6, HOXD1, and HOXD8 homeobox gene expression in human neuroblastoma cells following chemical induction of differentiation. Tumour Biol 1996; 17: 34-47.
[18] Liu H, Murthi P, Qin S, Kusuma GD, Borg AJ, Knofler M, Haslinger P, Manuelpillai U, Pertile MD, Abumaree M and Kalionis B. A novel combination of homeobox genes is expressed in mesenchymal chorionic stem/stromal cells in first trimester and term pregnancies. Reprod Sci 2014; 21: 1382-1394.
[19] Wang H, Huo X, Yang XR, He J, Cheng L, Wang N, Deng X, Jin H, Wang N, Wang C, Zhao F, Fang J, Yao M, Fan J and Qin W. STAT3-mediated upregulation of lncRNA HOXD-AS1 as a ceRNA facilitates liver cancer metastasis by regulating SOX4. Mol Cancer 2017; 16: 136.
[20] Li J, Zhuang C, Liu Y, Chen M, Chen Y, Chen Z, He A, Lin J, Zhan Y, Liu L, Xu W, Zhao G, Guo Y, Wu H, Cai Z and Huang W. Synthetic tetracycline-controllable shRNA targeting long non-coding RNA HOXD-AS1 inhibits the progression of bladder cancer. J Exp Clin Cancer Res 2016; 35: 99.
[21] Zheng L, Chen J, Zhou Z and He Z. Knockdown of long non-coding RNA HOXD-AS1 inhibits gastric cancer cell growth via inactivating the JAK2/STAT3 pathway. Tumour Biol 2017; 39: 1393384329.
[22] Gu P, Chen X, Xie R, Han J, Xie W, Wang B, Dong W, Chen C, Yang M, Jiang J, Chen Z, Huang J and Lin T. lncRNA HOXD-AS1 regulates proliferation and chemo-resistance of castration-resistant prostate cancer via recruiting WDR5. Mol Ther 2017; 25: 1959-1973.
[23] Yarmishyn AA, Batagov AO, Tan JZ, Sundaram GM, Sampath P, Kuznetsov VA and Kurochkin IV. HOXD-AS1 is a novel lncRNA encoded in HOXD cluster and a marker of neuroblastoma progression revealed via integrative analysis of noncoding transcriptome. Bmc Genomics 2014; 15: S7.
[24] Wang Q, Jiang S, Song A, Hou S, Wu Q, Qi L and Gao X. HOXD-AS1 functions as an oncogenic ceRNA to promote NSCLC cell progression by sequestering miR-147a. Onco Targets Ther 2017; 10: 4753-4763.
[25] Liu Z, Wei X, Zhang A, Li C, Bai J and Dong J. Long non-coding RNA HNF1A-AS1 functioned as an oncogene and autophagy promoter in hepatocellular carcinoma through sponging hsa-miR-30b-5p. Biochem Biophys Res Commun 2016; 473: 1268-1275.
[26] Liu XH, Sun M, Nie FQ, Ge YB, Zhang EB, Yin DD, Kong R, Xia R, Lu KH, Li JH, De W, Wang KM and Wang ZX. Lnc RNA HOTAIR functions as a competing endogenous RNA to regulate HER2 expression by sponging miR-331-3p in gastric cancer. Mol Cancer 2014; 13: 92.
[27] Yang H, Li Q, Niu J, Li B, Jiang D, Wan Z, Yang Q, Jiang F, Wei P and Bai S. microRNA-342-5p and miR-608 inhibit colon cancer tumorigenesis by targeting NAA10. Oncotarget 2016; 7: 2709-2720.
[28] Zheng J, Deng J, Xiao M, Yang L, Zhang L, You Y, Hu M, Li N, Wu H, Li W, Lu J and Zhou Y. A sequence polymorphism in miR-608 predicts recurrence after radiotherapy for nasopharyngeal carcinoma. Cancer Res 2013; 73: 5151-5162.
[29] Wang Z, Xue Y, Wang P, Zhu J and Ma J. MiR-608 inhibits the migration and invasion of glioma stem cells by targeting macrophage migration inhibitory factor. Oncol Rep 2016; 35: 2733-2742.
[30] Liang Z, Wang X, Xu X, Xie B, Ji A, Meng S, Li S, Zhu Y, Wu J, Hu Z, Lin Y, Zheng X, Xie L and Liu B. MicroRNA-608 inhibits proliferation of bladder cancer via AKT/FOXO3a signaling pathway. Mol Cancer 2017; 16: 96.

[31] Ueno K, Hirata H, Majid S, Yamamura S, Shahryari V, Tabatabai Z L, Hinoda Y and Dahiya R. Tumor suppressor microRNA-493 decreases cell motility and migration ability in human bladder cancer cells by downregulating RhoC and FZD4. Mol Cancer Ther 2012; 11: 244-253.

[32] Ma C, Xu B, Husaiyin S, Wang L, Wusainahong K, Ma J, Zhu K and Niyazi M. MicroRNA-505 predicts prognosis and acts as tumor inhibitor in cervical carcinoma with inverse association with FZD4. Biomed Pharmacother 2017; 92: 586-594.

[33] Lin J, Zandi R, Shao R, Gu J, Ye Y, Wang J, Zhao Y, Pertsemlidis A, Wistuba II, Wu X, Roth JA and Ji L. A miR-SNP biomarker linked to an increased lung cancer survival by miRNA-mediated down-regulation of FZD4 expression and Wnt signaling. Sci Rep 2017; 7: 9029.

[34] Gupta S, Iljin K, Sara H, Mpindi J P, Mirtti T, Vainio P, Rantala J, Alanen K, Nees M and Kallioniemi O. FZD4 as a mediator of ERG oncogene-induced WNT signaling and epithelial-to-mesenchymal transition in human prostate cancer cells. Cancer Res 2010; 70: 6735-6745.